ROS1 Signaling Regulates Epithelial Differentiation in the Epididymis

Hyun Jung Jun, Jeremy Roy, Tegan B. Smith, Levi B. Wood, Keara Lane, Steve Woolfenden, Diana Punko, Roderick T. Bronson, Kevin M. Haigis, Sylvie Breton, and Al Charest

Molecular Oncology Research Institute (H.J.J., S.W., D.P., A.C), Tufts Medical Center, Boston, Massachusetts 02111; Center for Cancer Research (K.L., A.C.), Massachusetts Institute of Technology, Cambridge, Massachusetts 02139; Program in Membrane Biology and Division of Nephrology and Center for Systems Biology (J.R., T.B.S., S.B.) and Molecular Pathology Unit (L.B.W., K.M.H.), Massachusetts General Hospital, Boston, Massachusetts 02114; Department of Pathology (R.T.B), Harvard Medical School, Boston, Massachusetts 02115; and Department of Neurosurgery and Program in Genetics (A.C), Tufts University School of Medicine, Boston, Massachusetts 02111

The initial segment (IS) of the epididymis plays an essential role in male fertility. The IS epithelium is undifferentiated and nonfunctional at birth. Prior to puberty, the epithelium undergoes differentiation that leads to the formation of a fully functional organ. However, the mechanistic details of this program are not well understood. To explore this further, we used genetic engineering to create a kinase dead allele of the ROS1 receptor tyrosine kinase in mice and studied the effects of ROS1 tyrosine kinase activity on the differentiation of the IS epithelium. We show that the expression and activation of ROS1 coincides with the onset of differentiation and is exclusively located in the IS of the maturing and adult mouse epididymides. Here we demonstrate that the differentiation of the IS is dependent on the kinase activity of ROS1 and its downstream effector MEK1/2-ERK1/2 signaling axis. Using genetic engineering, we show that germ line ablation of ROS1 kinase activity leads to a failure of the IS epithelium to differentiate, and as a consequence sperm maturation and infertility were dramatically perturbed. Pharmacological inhibition of ROS1 kinase activity in the developing epididymis, however, only delayed differentiation transiently and did not result in infertility. Our results demonstrate that ROS1 kinase activity and the ensuing MEK1/2-ERK1/2 signaling are necessary for the postnatal development of the IS epithelium and that a sustained ablation of ROS1 kinase activity within the critical window of terminal differentiation abrogate the function of the epididymis and leads to sterility. (*Endocrinology* 155: 3661–3673, 2014)

In mammals, spermatozoa produced in the testis are immature and gain motility and fertilizing capacity during their transit through the epididymis that provides an appropriate environment and supplies several of the molecules required for spermatozoa maturation (1–3). The epididymis is a single, highly convoluted tubule that is composed of a pseudostratified epithelial layer of several cell types (principal, basal, clear, and narrow cells) attached to a basement membrane and surrounded by contractile cells. The structure of the epididymis in a variety of species is functionally and structurally divided into four distinctive regions: initial segment (IS), caput, corpus, and cauda. The epididymal epithelial cells vary in number and size along the length of the epididymal duct and are equipped to perform specific functions. Each region expresses, synthesizes, and secretes a specific set of proteins resulting in unique luminal microenvironments that are essential for the sperm maturation process (4, 5).

At birth, the epididymis is still immature but continues to develop after birth with the differentiation of the epi-

ISSN Print 0013-7227 ISSN Online 1945-7170
Printed in U.S.A.

Received April 23, 2014. Accepted June 20, 2014.
First Published Online June 27, 2014

Abbreviations: AQP9, aquaporin 9; CASA, computer aided sperm analysis; ES, embryonic stem; IHC, immunohistochemistry; IS, initial segment; qRT-PCR, quantitative reverse transcription PCR.

thelial cells into principal, basal, and narrow/clear cells (5–10). At the onset of puberty and spermatogenesis, the epididymal epithelium develops segment-specific gene expression (5, 11) and gains regionalized functions aimed toward proper sperm concentration, maturation and storage. Genetic and experimental surgical studies demonstrated that the most proximal segments (IS and caput) are essential for sperm maturation because disrupted development or function often leads to male infertility (9, 12–19). Several lines of evidence revealed that the principal cells of the IS in postnatal, prepubescent mice require both testicular luminal fluid factors (or lumicrine factors) and androgen for terminal differentiation into fully functional, tall, columnar epithelial cells. However, there are still many unresolved issues regarding the signaling pathways that are responsible for the differentiation of the principal cells in the IS.

The orphan receptor tyrosine kinase ROS1 has a unique extracellular domain architecture composed of fibronectin type III repeat (FN-III) and beta propeller module (YWTD repeat) domains and an intracellular tyrosine kinase domain (reviewed in 20). The full-length ROS1 receptor is transiently expressed in various tissues during development and its pattern of expression during embryogenesis suggests that ROS1 initiates signaling events that are key components in the programmed differentiation of epithelial tissues (reviewed in Ref. 20). Deregulated ROS1 expression is also observed in many cancers. However its function remains poorly defined in normalcy and disease, mainly owing to a yet unidentified ligand.

To gain a better understanding of ROS1 function, mice with a constitutive deletion of the *Ros1* gene were generated (21). In these mice, complete ablation of the ROS1 receptor resulted in a gender and tissue-specific defect. Female homozygous ROS1 null mice do not display any detectable abnormalities, nor do heterozygous mice of either sex. Homozygous ROS1 null male mice, however, are infertile, but otherwise healthy. We have previously determined that the cause of infertility in these mice is the result of an epididymal epithelium differentiation defect that prevents spermatozoa from maturing during their passage through the epididymis (22). These studies revealed that complete absence of ROS1 receptor expression leads to a failure of IS epithelial differentiation.

The extracellular structure of ROS1 suggests that it may have a role in cell-to-cell signaling. Indeed, the *D. melanogaster* analog of ROS1, the Sevenless receptor, functions in a bidirectional manner. The extracellular domain of Sevenless serves as a ligand for the Bride of Sevenless receptor that is located on adjacent cells (23). Given the similarities between Sevenless and ROS1, it is likely that the extracellular domain of ROS1 also has biological functions. In the ROS1 receptor knockout study (21), the resulting phenotype could not be ascribed to either its extracellular or intracellular signaling functions. To study the tyrosine kinase activity and signaling pathways functions of ROS1 without affecting its extracellular role in vivo, we created a knock-in mutant kinase dead allele of ROS1 by replacing the ATP binding lysine residue to methionine, thereby eliminating ROS1 kinase activity without affecting other potential functions. Here we demonstrate the failure of the IS epithelium to differentiate in male mice carrying a kinase dead allele of ROS1, leading to sterility. Furthermore, we show through pharmacological means that ROS1 kinase activity and its MEK1/2 and ERK1/2 downstream signaling are necessary for differentiation of the IS during puberty but not for maintenance of epithelia integrity in the adult. Our results show that ROS1 kinase activity and its signaling pathways are necessary during a critical time for the proper differentiation of the principal cells of the IS in the mouse epididymis.

Materials and Methods

ROS1^{KM} knock-in targeting vector, gene targeting in embryonic stem (ES) cells, and derivation of ROS1^{KM} mice and genotyping

All mouse procedures were performed in accordance with Tufts University's recommendations for the care and use of animals and were maintained and handled under protocols approved by the Institutional Animal Care and Use Committee. We used recombineering methods (24–27) to generate a *Ros1* knock-in targeting vector and introduced the ROS1^{KM} mutant allele in ES cells through homologous recombination (Supplemental Materials and Methods). Positive ES clones produced founder animals to create the *ROS1^{tm1Char}* strain.

Immunoprecipitation, immunoblotting and immunofluorescence

Tissues lysates were separated by SDS-PAGE and transferred onto PVDF membrane (Immobilon P, Millipore), or immunoprecipitated using the indicated antibodies as described (Supplemental Materials and Methods). Immunofluorescence detection of aquaporin 9 (AQP9) labeling was performed on epididymis cryosections from the indicated ROS1 genotypes (Supplemental Materials and Methods). Epithelial height of the initial segment was calculated from 15 tubules from 2 separate animals to give a total of 30 tubules using Volocity software (version 6.3; Perkin Elmer). Care was taken to measure the epithelial height from tubules that were sectioned perpendicularly only.

Assessment of fertility

Adult males (10–12-weeks-old) of the indicated genotypes were each housed with adult wild-type females (6–10-weeks-old) for 4 days and the presence of a postcopulatory vaginal plug was recorded. Female mice were monitored for birth for 25 days. Mating was considered successful if one or more pups were born.

The reproductive rates (percentages) were calculated for each male and averaged.

Drug treatment

Crizotinib and PD325901 (LC Labs) were reconstituted in DMSO and diluted in Ora-Plus (Paddock) or PBS and administered by oral gavage or ip injection. Mice were treated with crizotinib (100 mg/kg oral gavage daily), PD325901 (20 mg/kg ip injection every 12 hours) or vehicle for the indicated periods of time as described (Supplemental Materials and Methods).

Sperm Analysis

Cauda epididymis spermatozoa were obtained by retrograde perfusion as described (28, 29) and either fixed with 2% paraformaldehyde for 15 minutes at 4°C, washed 3× in PBS to assess morphology or processed for computer aided sperm analysis (CASA) (Supplemental Materials and Methods).

Quantitative analysis of signaling

The caput (including the IS) was lysed using Bio-Plex cell lysis kit (Bio-Rad) and normalized in lysis buffer to 0.1 μg/μL using Pierce BCA (Thermo Scientific). Bio-Plex phospho-protein analysis was conducted using the Bio-Plex Phospho 13-Plex Assay (Bio-Rad) according to manufacturer's directions for analyzing tissue homogenate and described in details in Supplemental Materials and Methods.

Statistical analysis

Data were analyzed using GraphPad Prism (version 5; GraphPad Software Inc) using a two-tailed *t* test. Values are expressed as means ± SD or ± SEM as indicated.

Results

Generation of ROS1 K1973M kinase inactive knock-in mice

The overall architecture of ROS1 suggests that this receptor functions by linking extracellular cell adhesion to intracellular signaling. In addition, the extracellular domain of ROS1 may act as a ligand to a receptor located on adjacent cells. To study the effect of kinase inactivation without the loss of potential extracellular functions, we created a mouse strain using homologous recombination in mouse ES cells that carries a point mutant allele of the ROS1 gene that renders the receptor catalytically inactive. We previously showed that mutating the ATP binding lysine residue to methionine (K1973M) completely inactivates ROS1 tyrosine kinase activity (30). Using recombineering methods (24–27, 31–34), we created a *Ros1* K1973M ($ROS1^{KM}$) targeting vector (Supplemental Figure 1 and Materials and Methods) that was used to replace the endogenous *Ros1* locus by homologous recombination in ES cells (Figure 1A). Correct targeting and incorporation of the targeted allele into ES cells was confirmed by Southern blot analysis (Figure 1B). Targeted ES cells were used to generate germline-transmitting chimeras that were mated to create $ROS1^{KM/+}$ and $ROS1^{KM/KM}$ mice.

Structure and expression ROS1 in mouse tissues

The expression of ROS1 has been examined previously in chicken, mouse, rat, and human tissues in adults and at various stages of development by Northern blot analysis, RNase protection assays, and in situ hybridization (20, 35–38). Although informative, these techniques have limited sensitivities and a more thorough quantitative assessment of *Ros1* expression has never been undertaken. Using quantitative reverse transcription PCR (qRT-PCR) Taqman assays in 12 different adult mouse tissues, we determined that the expression of ROS1 transcripts in the adult is highly restricted with the highest levels observed in the epididymis and marginally in pancreatic and lung tissues (Supplemental Figure 2A). The mouse *Ros1* gene comprises 44 exons of which 34 code for the extracellular domain of the receptor and 10 encode for the intracellular kinase domain and COOH-terminal tail of the receptor. Whereas we have previously observed evidence of differential splicing of exons for human *ROS1* in different tissues (20), here we sought to delineate the structure of the mouse ROS1 receptor from the epididymis by purifying RT-PCR ROS1 mRNA fragments and aligning their sequences to the NCBI ROS1 Reference Sequence (NM_011282). Our analysis revealed the major epididymal ROS1 transcript is comprised of 44 exons coding for a full-length receptor with the addition to two low-abundance splice variants (Supplemental Figure 2, B and C).

In situ hybridization revealed that the highest levels of ROS1 expression in adult epididymides are restricted to the proximal epididymis, with the most robust hybridization detected in the initial segment and lower levels of ROS1 expression observed in the caput region (21). To confirm that the K1973M knock-in modification of the ROS1 locus does not affect expression of ROS1, we isolated total RNA from adult male proximal caput (including the IS), distal caput, corpus, and cauda epididymides from $ROS1^{+/+}$, $ROS1^{KM/+}$, and $ROS1^{KM/KM}$ mice and performed qRT-PCR assays. The ROS1 mRNA levels from all three genotypes were similar, confirming that the K1973M mutation does not alter the expression of mutant allele mRNA (Figure 1C). The expression of the $ROS1^{KM}$ allele was verified by direct sequencing of a RT-PCR fragment that spans the mutation. The $ROS1^{KM}$ mutant allele mRNA is equivalent to that of the wild-type allele (Figure 1D). These results correlate strongly with the presence of similar ROS1 receptor protein levels in $ROS1^{+/+}$, $ROS1^{KM/+}$, or $ROS1^{KM/KM}$ homozygous caput epididymides by Western blot (Figure 1E), with no detectable kinase activity of $ROS1^{KM/KM}$ as measured by the absence

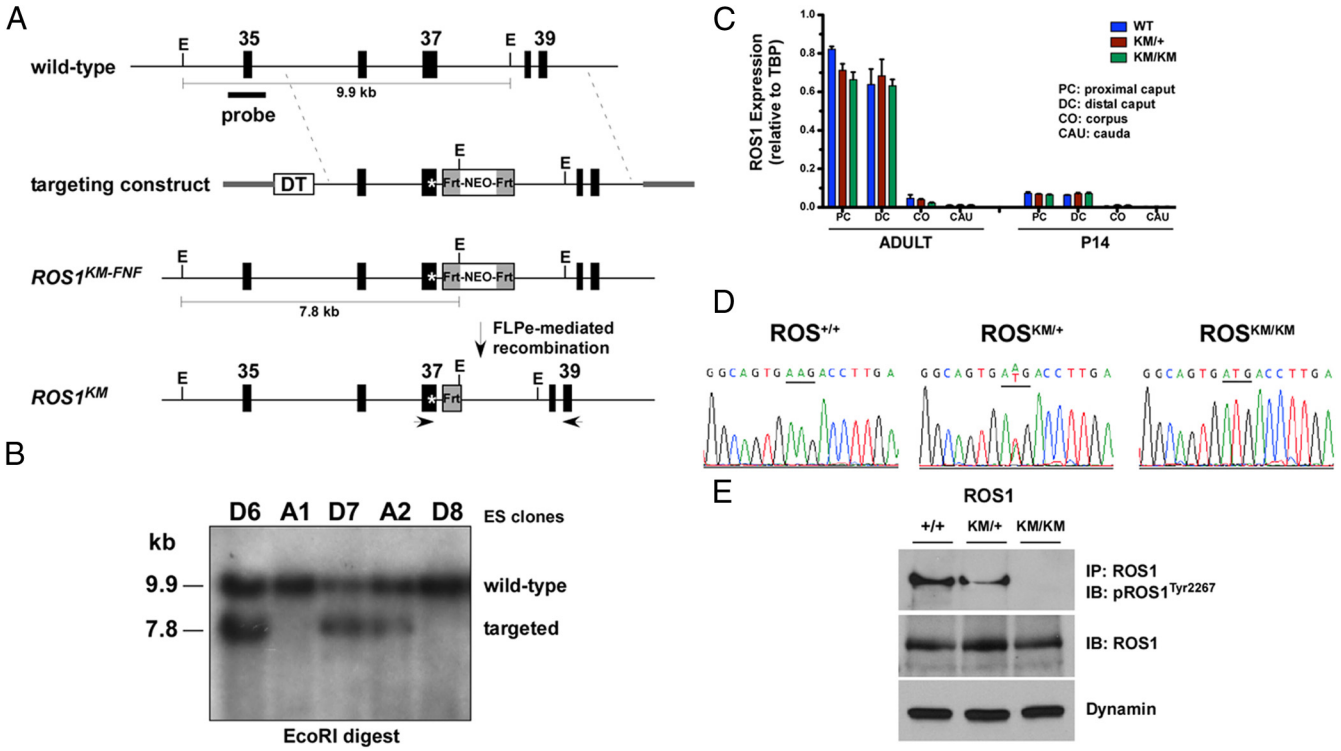

Figure 1. Schematic diagram of the K1973M targeting strategy. A, Diagram showing the composition of the endogenous mouse *Ros1* locus, the targeting vector, the knock-in allele resulting from homologous recombination and the recombined allele after excision of the Frt-NEO-Frt cassette. E indicates EcoRI restriction enzyme sites. Negative selection was achieved through DT at the 5′ end of the construct and positive selection was achieved through a neomycin resistance cassette (NEO). B, Southern blot analysis of EcoRI digested genomic DNA isolated from ES cells clones. The probe (Supplemental Materials and Methods) used for Southern blots is shown and detected a 9.9 kb WT fragment and a 7.8 kb targeted fragment. Clones D6, D7, and A2 contain the targeted allele. C, Relative expression of ROS1 in various regions of the adult and postnatal day 14 (P14) male epididymides of $ROS1^{+/+}$, $ROS1^{KM/+}$, and $ROS1^{KM/KM}$ genotypes. D, Chromatogram traces of sequencing reactions from an RT-PCR reaction from caput epididymis RNA isolated from the indicated ROS1 genotypes. E, Western blot analysis of caput epididymis extracts from the indicated genotypes. IP indicates immunoprecipitation, IB indicates immunoblot, p-ROS1 indicates phospho-$ROS1^{Tyr2267}$.

of phosphorylation at the autophosphorylation site Y2267 (Figure 1E). Collectively, these results demonstrate that the $ROS1^{KM}$ allele is expressed at similar levels to the wild-type allele in the caput epididymis and that $ROS1^{KM/KM}$ mice express a kinase inactive ROS1.

$ROS1^{KM/KM}$ mice are healthy

Mice carrying either one or two ROS1 KM alleles were viable and were born at expected Mendelian frequencies. The mice developed normally and exhibited no obvious behavioral or physical phenotype. We generated cohorts of $ROS1^{+/+}$ (n = 12), $ROS1^{KM/+}$ (n = 14), and $ROS1^{KM/KM}$ (n = 20) males and aged these animals for approximately 1 year (mean 357 days) to assess the role of ROS1 kinase activity in homeostasis. There was no difference in survival among mice with $ROS1^{+/+}$, $ROS1^{KM/+}$, and $ROS1^{KM/KM}$ knock-in genotypes, and gross anatomical analysis of these mice failed to reveal distinct phenotypes (data not shown).

Male mice null for the ROS1 receptor were previously documented to be sterile (21). We therefore tested whether the $ROS1^{KM}$ allele is essential for fertility. To investigate fertility, adult (10–12-weeks-old) $ROS1^{+/+}$, $ROS1^{KM/+}$, and $ROS1^{KM/KM}$ males were housed with adult wild-type females (6–10-weeks-old) for 4 days and the presence of a postcopulatory vaginal plug was recorded after which females were monitored for birth for 25 days. Each male was presented to >3 different females sequentially. Matings were scored as successful if one or more pups were born. $ROS1^{KM/KM}$ males sired no litters (Supplemental Table 1), unlike $ROS1^{+/+}$ and $ROS1^{KM/+}$ littermate controls (96.6% and 91.9% of matings resulting in live births respectively). These results demonstrate that loss of ROS1 kinase activity completely abolishes male fertility.

$ROS1^{KM/KM}$ sperm analysis

To determine the cause(s) of the observed infertility in $ROS1^{KM/KM}$ males, we isolated pure suspensions of spermatozoa from the caudal region of the epididymis and performed CASA. $ROS1^{KM/KM}$ males produced spermatozoa in comparable amounts to $ROS1^{+/+}$ males (data not shown), and consistent with the ROS1 knockout mouse (39), spermatozoa from the $ROS1^{KM/KM}$ displayed a hairpin morphology (Supplemental Figure 3, A, and B), making 66.7% of sperm observed when compared with 8.9%

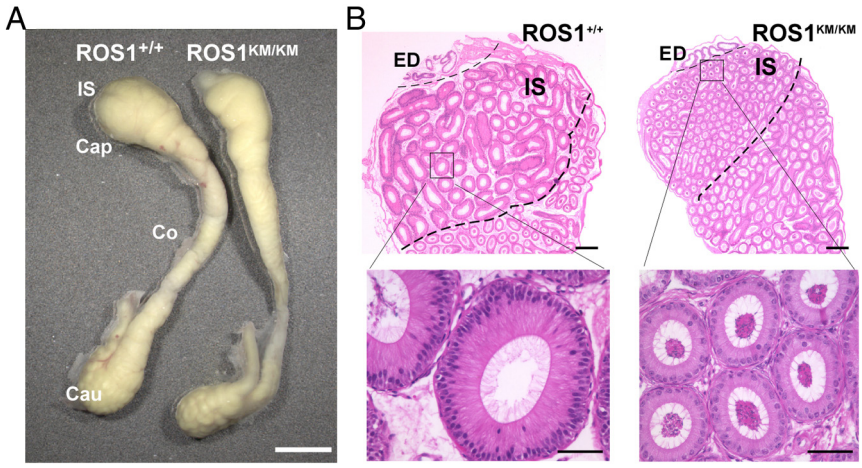

Figure 2. Kinase inactive ROS1 prevents epithelial cell differentiation of the initial segment epididymis. A, Photomicrograph of representative epididymides from ROS1$^{+/+}$ and ROS1$^{KM/KM}$. Note the atrophied caput region (Cap), whereas corpus (Co), and cauda (Cau) are comparable to controls. Scale bar, 2 mm. B, Photomicrographs of H&E-stained paraffin-embedded sections of adult male caput epididymides from ROS1$^{+/+}$ and ROS1$^{KM/KM}$ mice. Scale bars top panels, 250 μm; bottom panels, 25 μm. IS indicates initial segment, ED indicates efferent ducts.

in ROS1$^{+/+}$ (Supplemental Figure 3C). Nonsubjective CASA revealed a significant decrease in the progressive and total motility of ROS1$^{KM/KM}$ spermatozoa (Supplemental Figure 3D). To visualize the effects of the hairpin morphology on sperm motility, we recorded the movement characteristics of spermatozoa from ROS1$^{KM/KM}$ males. Aberrant motility was observed, in concert with little to no evidence of a normal straight morphology (Supplementary Movie).

Lack of ROS1 kinase activity prevents IS epithelia differentiation

We have previously demonstrated that the infertility phenotype originates from a deficiency in the IS epididymis to regulate luminal pH and osmolarity (22). This prompted us to investigate the anatomy of the epididymis in ROS1$^{KM/KM}$ adult animals. Gross morphology of ROS1$^{+/+}$ and ROS1$^{KM/KM}$ show that the ROS1$^{KM/KM}$ epididymides have a dysgenic proximal segment (Figure 2A). To examine this observation histologically, the proximal (IS and caput) epididymides were paraffin embedded and processed for histopathological analysis. As shown in Figure 2B, the atrophy observed in the ROS1$^{KM/KM}$ epididymides is restricted to the IS. Normal, fertile ROS1$^{+/+}$ initial segments are characterized by tall columnar fully differentiated epithelial cells, but as a consequence of the ROS1 kinase mutation, the height of columnar epithelial cells is reduced compared with the control (Figure 2B). To ascertain the extent of differentiation of the IS epithelium, cryostat sections of the caput epididymis were immunolabeled for the principal cell differentiation marker AQP9, and the height of principal cells in the IS was quantified. As shown in Figure 3, whereas a strong labeling was detected in the apical membrane of principal cells in the IS of adult ROS1$^{KM/+}$ (normal phenotype) mice, the region that corresponds to the IS in ROS1$^{KM/KM}$ mice did not stain positively for AQP9 (Figure 3A). In contrast, the efferent ducts were intensively labeled for AQP9 in both ROS1$^{KM/+}$ and ROS1$^{KM/KM}$ mice. In addition, the height of principal cells was significantly lower in ROS1$^{KM/KM}$ mice compared with ROS1$^{KM/+}$ mice (Figure 3B).

Puberty in mice is defined by full spermatogenic activity that occurs between 34 and 38 days postpartum. Prior to puberty, at day 17 to 21 days postpartum, the cuboidal IS epithelium differentiates into a tall columnar epithelium and gains enhanced secretory and absorptive features that are necessary for sperm maturation (for reviews see 4, 40). We determined using qRT-PCR and Western blotting that this process coincides with the expression of active ROS1 (Figure 4). Total RNA and protein were isolated from caput (including IS) epididymides from ROS1$^{+/+}$ mice 14, 21, 28, 35, 42, and 84 days postnatal, and ROS1 mRNA expression was measured by qRT-PCR (Figure 4A), and ROS1 receptor activity and expression were assessed by immunoblot analyses (Figure 4B). Our results demonstrate that ROS1 mRNA and active receptor proteins appear at the onset of differentiation of the IS between day 14 and 21 after birth expression and activity reaches its maximum level from postnatal day 28 (P28) onward.

Next, we determined if the process of differentiation from a nonfunctional cuboidal epithelium to a tall columnar epithelium in the IS is accompanied with changes in the cell cycle. We performed immunohistochemistry (IHC) on paraffin embedded sections of epididymal IS from ROS1$^{+/+}$ and ROS1$^{KM/KM}$ mice using Ki-67 staining (a marker of cells that have not entered G_0) (41) and demonstrated that there is a reduction in the number of Ki-67 positive cells in the IS between day 14 and 21 postnatal, with minimal Ki-67 positivity reached at day 28 onward for both ROS1$^{+/+}$ and ROS1$^{KM/KM}$ mice (Figure 4, C and D). This suggests that the observed exit from the cell cycle is not dependent on the kinase activity of ROS1 because the labeling index of Ki-67 in ROS1$^{KM/KM}$ is similar to that of ROS1$^{+/+}$ mice (Figure 4, C and D).

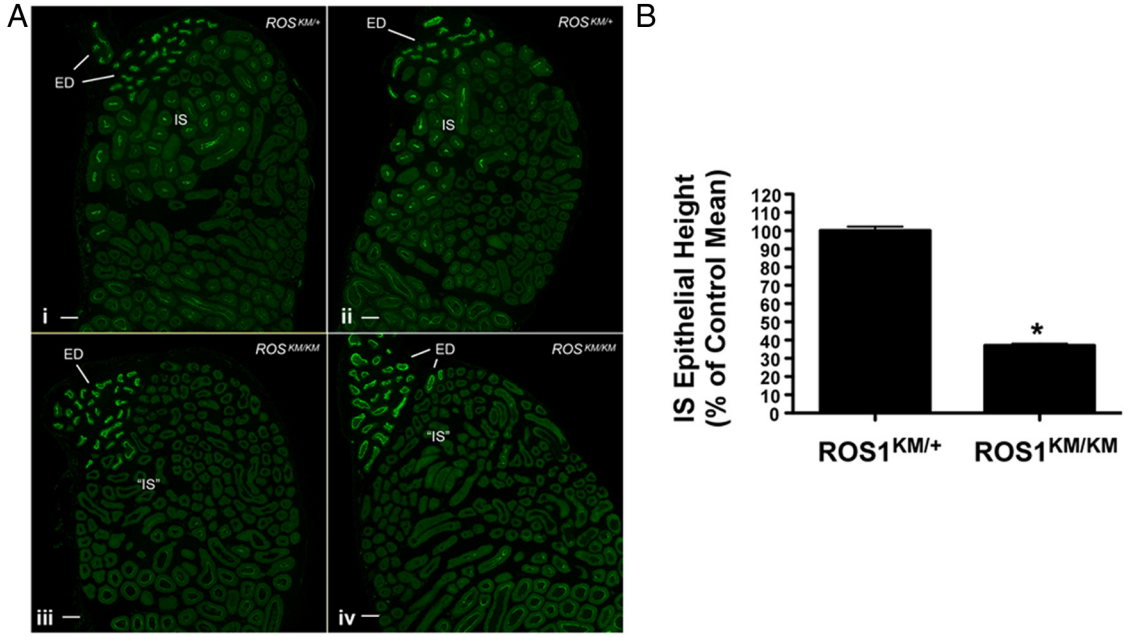

Figure 3. Terminal differentiation of principal cells is abrogated in ROS1$^{KM/KM}$ epididymides. A, Photomicrographs of anti-AQP9 immunofluorescence on 2 epididymides from ROS1$^{KM/+}$ normal (i and ii) and from ROS1$^{KM/KM}$ mutant mice (iii and iv). Strong AQP9 labeling is seen in the apical membrane of principal cells in the initial segment (IS) of ROS1$^{KM/+}$ mice. In contrast, AQP9 is not detectable in the corresponding segment (IS) of ROS1$^{KM/KM}$ mice. ED indicates efferent ducts. Bars, 100 μM. B, Quantification of the height of epithelial cells in the IS of normal mice and corresponding IS segment of mutant mice. Data are expressed as the average height from 15 tubules in 2 separate animals ± SEM. *, $P < .05$.

ROS1 signals through the MAPK pathway in the epididymis

It has been demonstrated that ROS1 signals through several downstream signaling pathways (20). We sought to quantitatively determine the effect of inactivating ROS1 kinase activity on signaling pathways using an unbiased phospho-proteomics approach (Bio-Plex). We performed a multiplex analysis of 12 phospho-signaling proteins

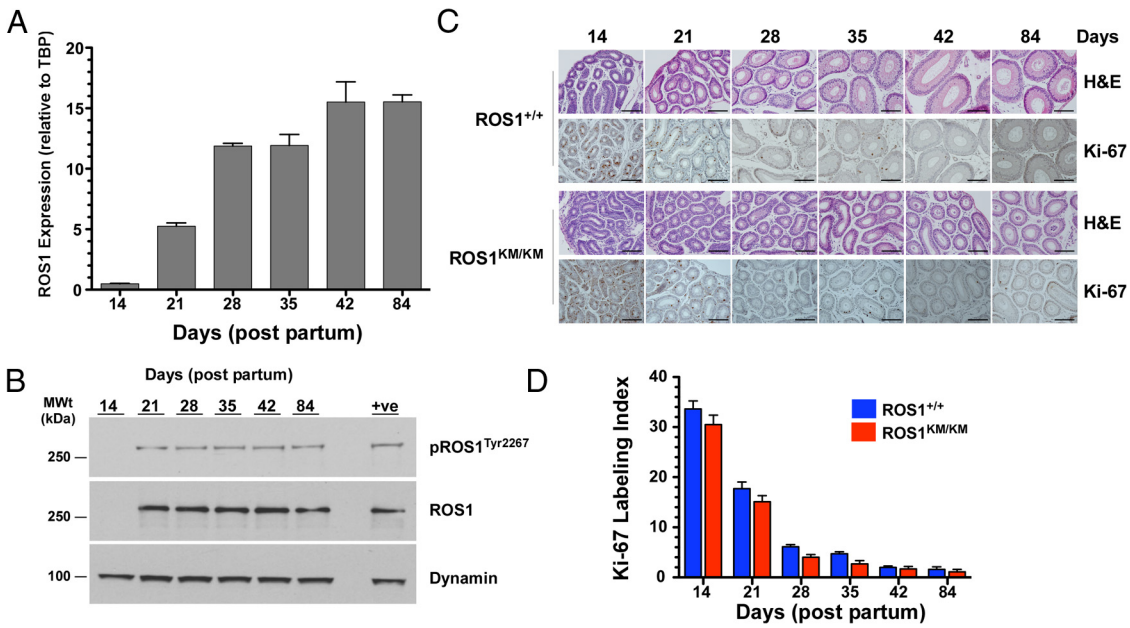

Figure 4. ROS1 expression coincides with the onset of differentiation. A, Levels of ROS1 mRNA expression from caput epididymides from males isolated at the indicated time points. B, Immunoblot analysis of caput epididymis extracts from males isolated at the indicated time points. The appearance of ROS1 protein coincides with the appearance of kinase active and autophosphorylated ROS1 (pTyr2267). C, The appearance of ROS1 expression and activation does not coincide with a decrease in the Ki-67 labeling index during development. IHC against Ki-67 marker in both ROS1$^{+/+}$ and ROS1$^{KM/KM}$ IS at the indicated time points. Scale bar, 500 μM. D, Quantification of the Ki-67 labeling index in ROS1$^{+/+}$ and ROS1$^{KM/KM}$ IS.

from pooled ROS1$^{+/+}$ and ROS1$^{KM/KM}$ caput epididymides (containing the IS). Our results demonstrate that a lack of ROS1 kinase activity results in a robust abrogation of the activation of the MEK1/2-ERK1/2 MAPK pathway (including phospho CREB(Ser133), phospho p90RSK(Ser380), and phospho STAT-3(Ser727) that are MEK-ERK targets) with little to no measurable effect on the AKT, p38 MAPK, and Src pathways (Figure 5A). We then validated the attenuated phospho MEK1/2-ERK1/2 levels observed in ROS1$^{KM/KM}$ by Western blot analysis on adult caput epididymides from ROS1$^{+/+}$, ROS1$^{KM/+}$, and ROS1$^{KM/KM}$ mice. Figure 5B shows that expression of kinase inactive ROS1 receptors has a drastic effect on the levels of phospho-MEK1/2 and phospho-ERK1/2 confirming the Bio-Plex results. We then performed IHC against phospho-ERK1/2 at different time points during epididymal development to determine the if the appearance of MEK1/2-ERK1/2 signaling coincides with the onset of ROS1 expression that we have shown to be between P14 and P21 (Figure 4). We show that not only phospho-ERK1/2 staining appears between P14 and P21 in ROS1$^{+/+}$ IS but that it is completely absent from ROS1$^{KM/KM}$ IS, further validating our Bio-Plex and Western blot results (Figure 5C).

Transient pharmacological inhibition of ROS1 signaling delays differentiation without affecting fertility

Having demonstrated that genetic inactivation of ROS1 kinase function results in a failure of the epididymal epithelium to fully differentiate, we questioned if inhibition of ROS1 through pharmacological means at defined time points during the process of differentiation could yield a similar outcome. Phylogenically, ROS1 is a distinct kinase that is closely related to the ALK receptor suggesting that inhibitors of ALK may have efficacy against ROS1. To inhibit ROS1 kinase activity in vivo, we used crizotinib (Xalkori), an FDA-approved ALK/MET inhibitor that we have previously shown to potently cross-react with ROS1 (42). We first determined the profile of ALK and MET mRNA expression from 12 adult mouse tissues

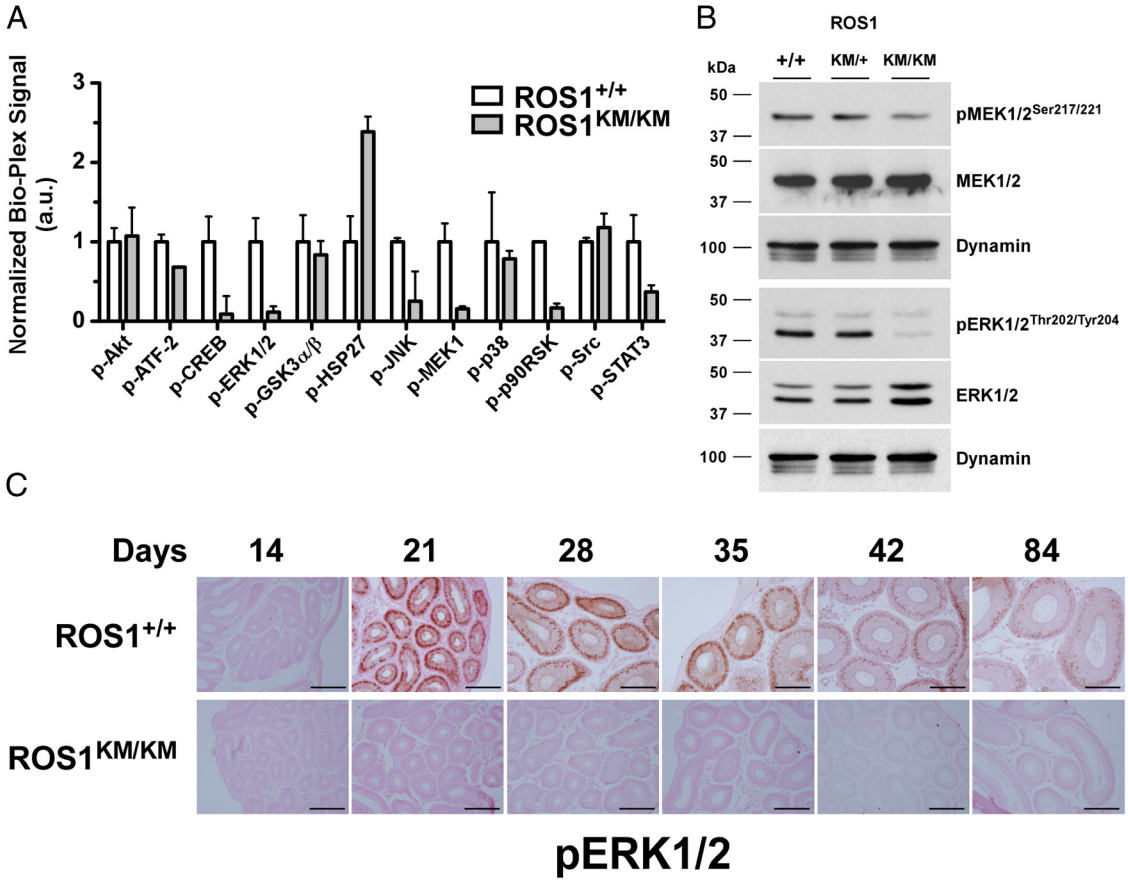

Figure 5. MEK/ERK signaling in the caput epididymis (including IS) is reduced in ROS1 kinase dead mice. A, Quantitative measurements of signaling network members by multiplex phosphoproteomics (Bio-Plex). Lysates from ROS1$^{+/+}$ and ROS1$^{KM/KM}$ caput epididymides were subjected to quantitative multiplex phospho proteomic analysis using Bio-Plex. Results are reported as arbitrary units (a.u.) relative to ROS1$^{+/+}$. B, The levels of phospho MEK1/2 and phospho ERK1/2 were measured by Western blot analysis of caput epididymis extracts from ROS1$^{+/+}$, ROS1$^{KM/+}$, and ROS1$^{KM/KM}$ mice. C, The appearance of phospho-ERK1/2 protein coincides with the onset of ROS1 expression and activation in ROS1$^{+/+}$ but not in ROS1$^{KM/KM}$ mice. Scale bar, 500 μM.

using qRT-PCR and showed that ALK mRNA is not detected in the epididymis and that MET is marginally expressed (Supplemental Figure 4A). To determine the extent of ALK and MET expression, we performed qRT-PCR reactions on RNA isolated from microdissected caput epididymis (including IS and caput) tissues at various time points during epididymal development. We found that ALK is not detectable and that MET expression remains at low levels during proximal epididymal development (Supplemental Figure 4B). In contrast, ROS1 expression increases dramatically at the time of IS differentiation. We then confirmed that the low level of MET mRNA expression does not yield detectable levels of MET receptor and activated phospho-MET receptors as observed by Western blotting (Supplemental Figure 4C). Finally, we determined using Western blotting and IHC that maximal epididymal ROS1 inhibition with crizotinib in adult mice is attained after 5 days of treatments daily po at 100 mg/kg (Supplemental Figure 5).

To study the consequences of pharmacological inhibition of ROS1 kinase activity during the onset of IS epithelium differentiation, we administered crizotinib daily by oral gavage (100 mg/kg) in prepubescent P17 pups, and harvested epididymides 5 and 12 days later (at P21 and P28 respectively). Treatment of mice with crizotinib efficiently inhibited ROS1 kinase activity in epididymides as measured by a complete absence of phospho-ROS1^{Tyr2267} (Figure 6A). Furthermore, inhibition of ROS1 kinase activity efficiently eliminated phospho-ERK1/2 proteins (Figure 6A). Within the time frame of observation, the inhibition of ROS1 kinase activity by crizotinib prevented the differentiation of the IS, which paralleled the elimination of MEK1/2-ERK1/2 signaling as observed by a decrease in the levels of phospho-ERK1/2 measured by IHC (Figure 6B). These results demonstrate that drug-induced inhibition of ROS1 during the critical period of the onset of differentiation leads to abrogation of MEK1/2-ERK1/2 signaling within the IS and a failure to induce epithelial differentiation.

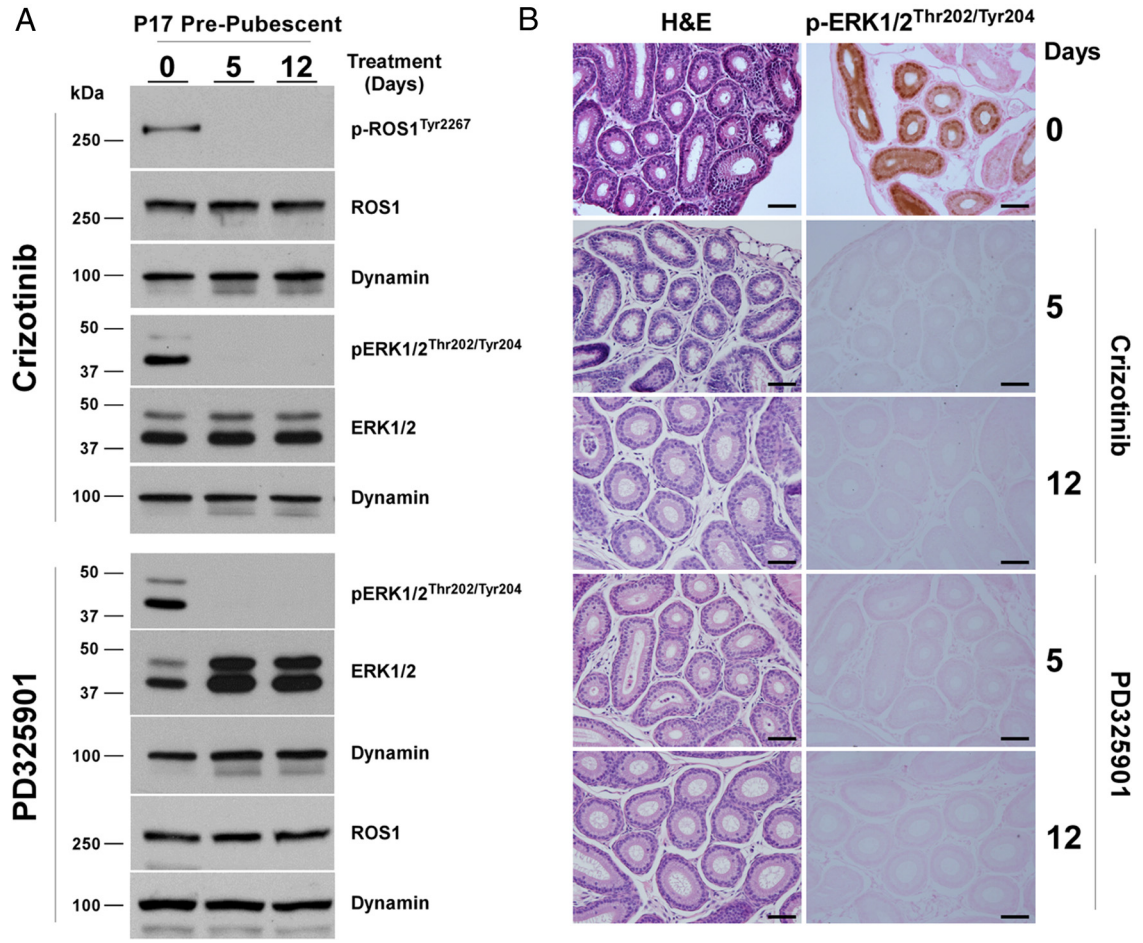

Figure 6. Pharmacological inhibition of ROS1 or MEK1/2 in prepubescent mice prevents IS epithelia differentiation. A, Western blot analysis of lysates from caput epididymides from ROS1 wild-type mice treated with either crizotinib or PD325901 for 0, 5, and 12 days against the indicated proteins. B, Photomicrographs of paraffin-embedded sections from caput epididymides of (A) stained with H&E or for expression of phospho-ERK1/2 by IHC. Scale bar, 250 μm.

Given our results demonstrating a robust use of the MEK/ERK pathway by ROS1 in the IS, we ascertained if inhibition of MEK1/2 directly could phenocopy the effect of ROS1 inhibition. We administered P17 male pups with the MEK1/2 inhibitor PD325901 (20 mg/kg IP every 12 hours) for 5 and 12 days and harvested epididymides at P21 and P28, respectively. Treatment of mice with PD325901 efficiently inhibited MEK1/2 kinase activity in epididymides as measured by a complete absence of phospho-ERK1/2, however the expression of ROS1 was not affected (Figure 6A). In addition, the inhibition of MEK1/2 kinase activity by PD325901 prevented the differentiation of the IS epithelium that paralleled the elimination of phospho-ERK1/2 levels as measured by IHC (Figure 6B). These results demonstrate that drug-mediated inhibition of MEK1/2 at the time of differentiation leads to abrogation of MEK1/2-ERK1/2 signaling within the IS, resulting in a failure to induce epithelial differentiation.

To determine the long-term effects of transient peripubertal ROS1 inhibition on the structure and function of the adult IS, we ascertained the differentiation status of the IS epithelium by measuring epithelial height, and we performed fertility tests on 10-week-old adult (P70) males that had been treated with crizotinib for 12 days during the critical period of differentiation (between P17–P28) as above. We found that the levels of phospho-ROS1^{Tyr2267} (ie, ROS1 kinase activity) returned to normal level within 42 days after cessation of crizotinib treatment (Figure 7A) that correlated with a rectification of the IS epithelium height (Figure 7B). In addition, transient crizotinib treatment during the prepuberty phase in these animals did not affect their fertility once they reached adulthood (Figure 7C). Taken together, these results suggest that transient inhibition of ROS1 kinase activity during prepuberty transiently delays a differentiation program and that only sustained ROS1 inhibition (as in the ROS1$^{KM/KM}$ mice) leads to a sustained lack of IS differentiation with a persistent infertility phenotype.

Pharmacological inhibition of ROS1 kinase activity in adults does not affect fertility

Finally, we also investigated if inhibition of ROS1 kinase activity had an effect on the architecture of the IS epithelium in adult mice, where terminal differentiation of the IS epithelia has already occurred. Adult mice (10-weeks-old) were treated with crizotinib for 7 or 14 days and the levels of phospho-ROS1^{Tyr2267} were measured by Western blot analysis (Figure 8A). After 7 days of treatment, ROS1 activity was completely abrogated, which corresponded with a marked decrease in the levels of phospho-ERK1/2. After 14 days of treatment, the levels of phospho-ROS1^{Tyr2267} remained attenuated but the levels of phospho-ERK1/2 returned to those of untreated control epididymides (Figure 8A). Pharmacological inhibition of ROS1 kinase activity during prepuberty blocked the differentiation of the IS epithelium that was accompanied by a decrease in the levels of phospho-ERK1/2 staining by IHC (Figure 6B). On the other hand, inhibiting ROS1 kinase activity in adults had no consequences on the architecture of the IS epithelium, despite completely eliminating the levels of phospho-ERK1/2 after 7 days as detected by IHC (Figure 8B). Interestingly, we noticed that the reap-

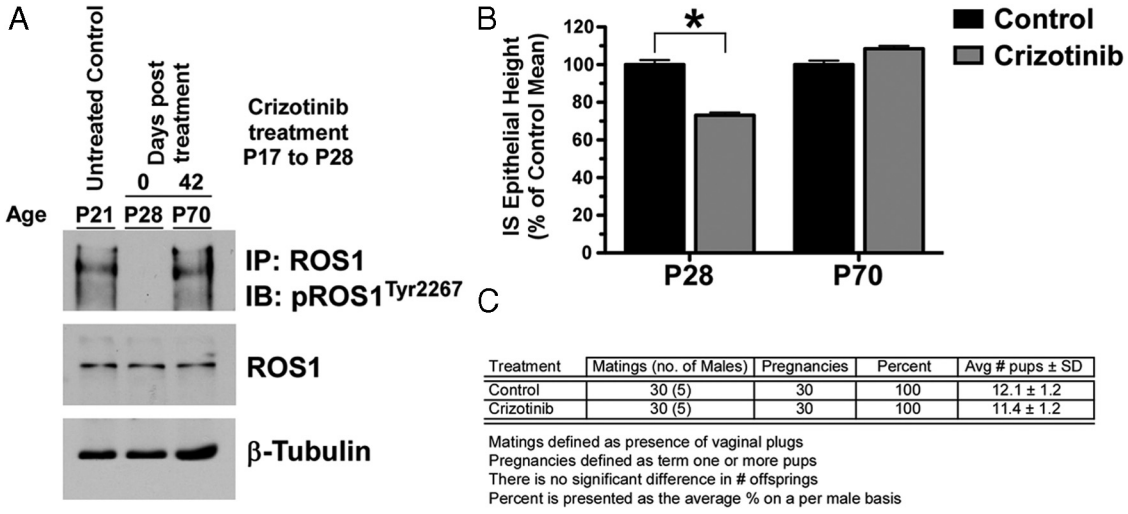

Treatment	Matings (no. of Males)	Pregnancies	Percent	Avg # pups ± SD
Control	30 (5)	30	100	12.1 ± 1.2
Crizotinib	30 (5)	30	100	11.4 ± 1.2

Matings defined as presence of vaginal plugs
Pregnancies defined as term one or more pups
There is no significant difference in # offsprings
Percent is presented as the average % on a per male basis

Figure 7. Peripubertal inhibition of ROS1 kinase activity has no long-term effect on architecture of IS epithelium and fertility. A, Western blot analysis of caput (including IS) from males that were treated with crizotinib between P17 to P28 and aged to P70 for the levels of phospho-ROS1. P21 untreated caput epididymides were used as a positive control. B, The heights of IS epithelium were measured in 2 control and 2 crizotinib-treated (from P17 to P28) in juvenile males immediately posttreatment (P28) and 42 days after cessation of treatment (P70 adult). *, $P < .05$. C, Peripubertal crizotinib-treated and control mice (N = 5 each) as in (B) were aged to adulthood (10-weeks-old) and mated with 6-week-old females. Copulatory vaginal plugs and pregnancies were recorded and percent fertility calculated as the number of pregnancy/plugs.

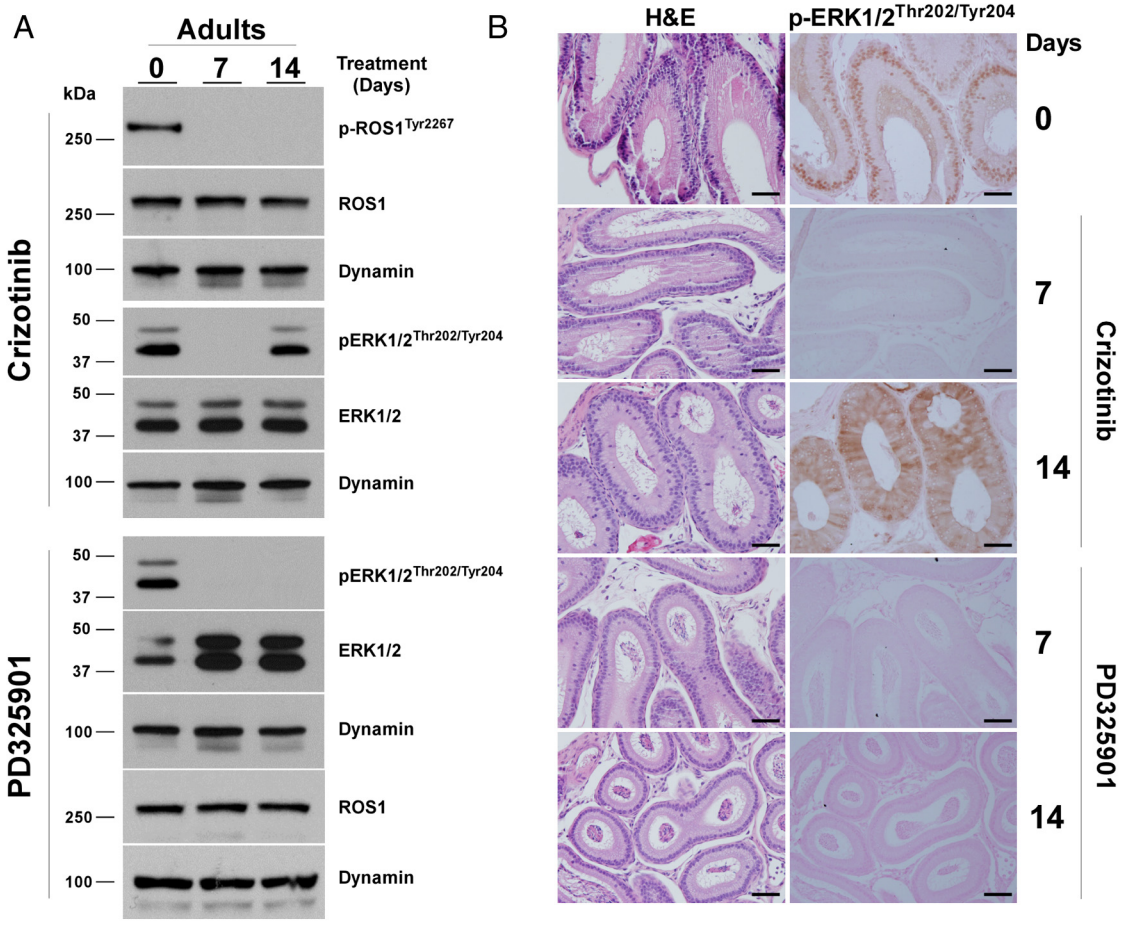

Treatment	Matings (no. of Males)	Pregnancies	Percent
Control	30 (5)	30	100
Crizotinib	36 (6)	36	100

Matings defined as presence of vaginal plugs
Pregnancies defined as term one or more pups
Percent is presented as the average % on a per male basis

Figure 8. Inhibition of ROS1 and MEK1/2 kinase activity in adults. A, Western blot analysis of lysates from caput epididymides (including IS) from ROS1 wild-type mice treated with either crizotinib or PD325901 for 0, 7, and 14 days against the indicated proteins. B, Photomicrographs of paraffin-embedded sections from proximal epididymides treated as per (A) and stained with H&E or phospho-ERK1/2 by IHC. Scale bar, 250 μm. C, Western blot analysis of lysates from proximal caput epididymides (including IS) from ROS1 wild-type mice treated with crizotinib for 12 days. D, Crizotinib-treated and control mice were mated with 6-week-old females and copulatory vaginal plugs and pregnancies were recorded, and percent fertility calculated from the number of pregnancy/plugs.

pearance of phospho-ERK1/2 after prolonged ROS1 inhibition with crizotinib (14 days) was localized mainly to the cytoplasm, as opposed to a mostly nuclear localization in control tissues (Figure 8B). Similarly, PD325901 treatment inhibition of MEK1/2 post puberty in adult animals for 7 and 14 days efficiently down-regulated the MEK1/2-ERK1/2 signaling without affecting ROS1 expression (Figure 8A) and the architecture of the IS epithelium was not affected (Figure 8B). Similar to ROS1 inhibition in adults, inhibition of MEK with PD325901 in adults demonstrates that a ROS1-MEK/ERK signaling axis is not necessary for maintenance of the IS epithelia architecture.

Although no architectural defect in the IS epithelium was noticed in adult mice, we were curious as to whether

transient pharmacological inhibition of ROS1 could alter its function. We treated adult $ROS1^{+/+}$ males with crizotinib for 12 days and tested their fertility as above. Although ROS1 kinase activity was completely eliminated (Figure 8C), crizotinib treated $ROS1^{+/+}$ males were comparably fertile to nontreated control animals (Figure 8D). Together these results suggest that transient ROS1 kinase inhibition using a pharmacological agent in adult males has no effects on the architecture of the IS epithelium, or on the fertility of treated animals.

Discussion

From birth to adulthood, the postnatal epididymal development can be divided into three stages. The first stage is known as the undifferentiated period where the cells of the epididymal epithelium are characterized by the presence of low columnar or cuboidal undifferentiated cells that lack stereocilia, and are still engaged in proliferation as they contain multiple mitotic figures (9). In mice, this period corresponds to P1 to P17. Our analysis of ROS1 expression by qRT-PCR and Western blots from P14 epididymides demonstrates that both ROS1 message and protein are absent from this stage and that MEK1/2-ERK1/2 usage is minimal. Ki-67 proliferation index is highest, suggesting that ROS1 is not involved in the proliferation of these nondifferentiated epithelial cells.

The second stage is a period of differentiation in which the epididymal epithelium begins to differentiate and several different cell types begin to appear including principal, narrow/clear, and basal cells, and the four structural regions of the epididymis (IS, caput, corpus, and cauda) begin to emerge and function (43). During this period, principal cells of the IS terminally differentiate from low columnar to tall columnar and acquire a distinctive Golgi apparatus, long stereocilia, and several vesicles and coated pits, indicative of active endocytosis. In rats, a marked increase in several markers of principal cell differentiation, including aquaporins 2, 5, 7, 9, and 11 is initiated during the second postnatal week in epithelial cells isolated by laser capture microdissection (8). Narrow and clear cells, as well as basal cells also start to differentiate during this period (10, 44). In mice, this differentiation period corresponds to P17 to P44. Here we demonstrate that the Ki-67 proliferative index decreases dramatically during this stage, consistent with cells exiting the cell cycle and entering a G_0 postmitotic differentiated stage. We also show that the expression and activation of the full-length ROS1 receptor coincides with this period, and ROS1 and MEK1/2 activities are essential for the differentiation of IS principal cells.

The third period corresponds to a postdifferentiation stage and is mostly expansionary. The most significant changes associated with this stage are the appearance of spermatozoa within the epididymal lumen and an increase in size and length of the epididymis. In addition, proliferation of all cell types has ceased throughout the epididymal epithelium at this stage (9, 45), which we also observed in both $ROS1^{+/+}$ and $ROS1^{KM/KM}$ mice. In the mouse, this period is from P44 to adulthood. We find that ROS1 is expressed and active in the IS at this stage and that inhibition of ROS1 or MEK1/2 through pharmacological means in adult animals had little impact on the overall architecture of the IS epithelium and the function of the epididymis, as measured by no changes in fertility. These results combined suggest that activation of ROS1 is necessary to induce a differentiation program and does not seem to have a direct role in cell proliferation in epididymal tissues.

It has previously been demonstrated that abrogation of epithelial differentiation in the IS leads to physiological defects in regulating pH and osmolarity of epididymal fluids, resulting in immature spermatozoa that are incapable of regulating their cellular volume (22, 39, 46, 47). Consequently, sperm transiting through such a defective epididymis do not mature and interestingly, take on a hairpin phenotype and have reduced motility. Similar to the full ROS1 knockout mouse, this marked motility decline likely results in the inability of the spermatozoon to enter the oviduct, and their bent tails thus compromise flagellar vigor within the uterus (39, 47).

Elegant studies on the activation of the ERK1/2 in the caput epididymis revealed that there are two activity levels of the ERK1/2 pathway. A basal level of ERK1/2 activity is observed throughout the entire length of the epididymis prior to the period of differentiation and in most epithelial cells post differentiation, except for the IS epithelium (48–50). A second, much higher level of ERK1/2 activity has been observed only in the IS epithelium from P17 onward (49) that we found coincides with the appearance of ROS1 receptor activity. Indeed, we demonstrate that this high level of ERK1/2 activation is completely abolished in the IS of our $ROS1^{KM/KM}$ animals and in the pharmacologically inhibited ROS1 and MEK1/2 mice. This high ERK1/2 activation in the P17–P44 IS has also been shown to be induced by the onset or appearance of lumicrine factors in the IS (48, 49), possibly suggesting that one of the lumicrine factors is a ligand for ROS1, and is responsible for its activation and ensuing signaling through ERK1/2.

Our results indicate that ROS1 and MEK1/2-ERK1/2 signaling in the developing IS epithelium promotes differentiation. This is in stark contrast to constitutively acti-

vated oncogenic ROS1 fusion kinases that also signal through MEK1/2-ERK1/2 pathways and that have been shown to lead to proliferative signaling rather than differentiation (42). One important question that remains unanswered is how can activation of a well-known mitogenic signaling pathway such as ROS1-MEK1/2-ERK1/2 lead to a differentiation program rather than the induction of proliferation?

It is possible that in IS epithelia, ROS1 activates parallel yet unidentified signals that mitigate the promitotic effects of MEK1/2-ERK1/2 or redirect MEK1/2-ERK1/2 signaling to a prodifferentiation outcome. For example, we know that in cancer, ROS1 activation also turns on proliferative and survival signals such as the PI3K-AKT-mTORC signaling axis that perhaps dominates over weaker prodifferentiation signals (51). Using a quantitative measurement of signaling molecules approach (Bio-Plex) we show that indeed p-AKT(Thr308) is unaffected in the $ROS1^{KM/KM}$ epididymides, suggesting that ROS1 signaling in this tissue does not activate an AKT centric pathway. Alternatively, the cellular context in which ROS1 signaling occurs may very well be responsible for these seemingly dichotomic actions of MEK1/2-ERK1/2. In fact, epididymal tumors are extremely rare, perhaps reflecting a nonconducive disposition for this tissue to transformation whereas most oncogenes use a MEK1/2-ERK1/2 centric signaling pathway to convey their oncogenicity.

In conclusion, we show that the kinase activity of ROS1 is indispensable for triggering MEK1/2-ERK1/2 driven differentiation signals during a crucial period of the caput epididymides postnatal development. Our genetic experiments were validated with pharmacological approaches and reveal the sensitive and transient nature of epithelial dependency on ROS1 signaling events for the induction of a differentiation program. The work described here reinforces the importance of a properly functioning IS for the maturation of spermatozoa and our results hint at the limitations to short term targeting of ROS1 kinase activity in adults as a potential male contraceptive.

Acknowledgments

The authors thank Drs Vicky Appleman and Katy Wong for their critical review of the manuscript and Professor David Housman from the Massachusetts Institute of Technology in whose laboratory this work was initiated.

Address all correspondence and requests for reprints to: Alain Charest, Tufts Medical Center, MORI, 800 Washington St, box 5609, Boston, MA 02111; E-mail: alain.charest@tufts.edu.

The current address for K. L. is Department of Bioengineering, Stanford University, Stanford, CA 94305.

This work was supported by National Institutes of Health Grants NCI U01 CA141556 (to A.C.) and RO1 DK085715–05 (to S.B.), the American Cancer Society Research Scholar Award 117409 (to A.C.), and by the Massachusetts General Hospital Charles and Ann Sanders Research Scholar Award.

Disclosure Summary: The authors have nothing to disclose.

References

1. **Orgebin-Crist M-C, Danzo BJ, Davies J.** 1975 Endocrine control of the development and maintenance of sperm fertilizing ability in the epididymis. In: Hamilton DW, Greep RO, eds. Handbook of physiology. Washington DC: American Physiological Society; 319–338.
2. **Bedford JM.** 1975 Maturation, transport and fate of spermatozoa in the epididymis. In: Hamilton DW, Greep RO, eds. Handbook of physiology. Washington DC: American Physiological Society; 303–317.
3. **Hinton BT.** 1995 What does the epididymis do and how does it do it? In: Hinton BT, Robaire B, Prryor JL, Trasler JM, eds. Handbook of andrology. Lawrence: American Society of Andrology; 1–5.
4. **Cornwall GA.** New insights into epididymal biology and function. *Hum Reprod Update*. 2009;15:213–227.
5. **Robaire B, Syntin P, Jervis K.** 2000 The coming of age of the epididymis. In: Jegou B, ed. Testis, epididymis and technologies in the year 2000. New York: Springer-Verlag; 229–262.
6. **Hermo L, Barin K, Robaire B.** Structural differentiation of the epithelial cells of the testicular excurrent duct system of rats during postnatal development. *Anat Rec*. 1992;233:205–228.
7. **Sun EL, Flickinger CJ.** Development of cell types and of regional differences in the postnatal rat epididymis. *Am J Anat*. 1979;154:27–55.
8. **Da Silva N, Silberstein C, Beaulieu V, et al.** Postnatal expression of aquaporins in epithelial cells of the rat epididymis. *Biol Reprod*. 2006;74:427–438.
9. **Rodriguez CM, Kirby JL, Hinton BT.** 2002 The development of the epididymis. In: Robaire B, Hinton BT, eds. The epididymis: from molecules to clinical practice. New York: Kluwer Academic/Plenum Publishers; 251–267.
10. **Shum WW, Hill E, Brown D, Breton S.** Plasticity of basal cells during postnatal development in the rat epididymis. *Reproduction*. 2013;146:455–469.
11. **Kirchhoff C.** Gene expression in the epididymis. *Int Rev Cytol*. 1999;188:133–202.
12. **Bjorkgren I, Saastamoinen L, Krutskikh A, Huhtaniemi I, Poutanen M, Sipila P.** Dicer1 ablation in the mouse epididymis causes dedifferentiation of the epithelium and imbalance in sex steroid signaling. *PLoS One*. 2012;7:e38457.
13. **Krutskikh A, De Gendt K, Sharp V, Verhoeven G, Poutanen M, Huhtaniemi I.** Targeted inactivation of the androgen receptor gene in murine proximal epididymis causes epithelial hypotrophy and obstructive azoospermia. *Endocrinology*. 2011;152:689–696.
14. **O'Hara L, Welsh M, Saunders PT, Smith LB.** Androgen receptor expression in the caput epididymal epithelium is essential for development of the initial segment and epididymal spermatozoa transit. *Endocrinology*. 2011;152:718–729.
15. **Sipilä P, Cooper TG, Yeung CH, et al.** Epididymal dysfunction initiated by the expression of simian virus 40 T-antigen leads to angulated sperm flagella and infertility in transgenic mice. *Mol Endocrinol*. 2002;16:2603–2617.
16. **McPhaul MJ.** Androgen receptor mutations and androgen insensitivity. *Mol Cell Endocrinol*. 2002;198:61–67.

17. **Mendive F, Laurent P, Van Schoore G, Skarnes W, Pochet R, Vassart G.** Defective postnatal development of the male reproductive tract in LGR4 knockout mice. *Dev Biol*. 2006;290:421–434.
18. **Hoshii T, Takeo T, Nakagata N, Takeya M, Araki K, Yamamura K.** LGR4 regulates the postnatal development and integrity of male reproductive tracts in mice. *Biol Reprod*. 2007;76:303–313.
19. **Murashima A, Miyagawa S, Ogino Y, et al.** Essential roles of androgen signaling in Wolffian duct stabilization and epididymal cell differentiation. *Endocrinology*. 2011;152:1640–1651.
20. **Acquaviva J, Wong R, Charest A.** The multifaceted roles of the receptor tyrosine kinase ROS in development and cancer. *Biochim Biophys Acta*. 2009;1795:37–52.
21. **Sonnenberg-Riethmacher E, Walter B, Riethmacher D, Gödecke S, Birchmeier C.** The c-ros tyrosine kinase receptor controls regionalization and differentiation of epithelial cells in the epididymis. *Genes Dev*. 1996;10:1184–1193.
22. **Yeung CH, Breton S, Setiawan I, Xu Y, Lang F, Cooper TG.** Increased luminal pH in the epididymis of infertile c-ros knockout mice and the expression of sodium-hydrogen exchangers and vacuolar proton pump H+-ATPase. *Mol Reprod Dev*. 2004;68:159–168.
23. **Raabe T.** The sevenless signaling pathway: variations of a common theme. *Biochim Biophys Acta*. 2000;1496:151–163.
24. **Thomason L, Court DL, Bubunenko M, et al.** 2007 Recombineering: genetic engineering in bacteria using homologous recombination. *Curr Protoc Mol Biol*. 2007;Chapter 1:Unit1.16.
25. **Court DL, Swaminathan S, Yu D, et al.** Mini-lambda: a tractable system for chromosome and BAC engineering. *Gene*. 2003;315:63–69.
26. **Court DL, Sawitzke JA, Thomason LC.** Genetic engineering using homologous recombination. *Annu Rev Genet*. 2002;36:361–388.
27. **Copeland NG, Jenkins NA, Court DL.** Recombineering: a powerful new tool for mouse functional genomics. *Nat Rev Genet*. 2001;2:769–779.
28. **Smith TB, Baker MA, Connaughton HS, Habenicht U, Aitken RJ.** Functional deletion of Txndc2 and Txndc3 increases the susceptibility of spermatozoa to age-related oxidative stress. *Free Radic Biol Med*. 2013;65:872–881.
29. **Smith TB, De Iuliis GN, Lord T, Aitken RJ.** The senescence-accelerated mouse prone 8 as a model for oxidative stress and impaired DNA repair in the male germ line. *Reproduction*. 2013;146:253–262.
30. **Charest A, Kheifets V, Park J, et al.** Oncogenic targeting of an activated tyrosine kinase to the Golgi apparatus in a glioblastoma. *Proc Natl Acad Sci USA*. 2003;100:916–921.
31. **Rodríguez CI, Buchholz F, Galloway J, et al.** High-efficiency deleter mice show that FLPe is an alternative to Cre-loxP. *Nat Genet*. 2000;25:139–140.
32. **Sharan SK, Thomason LC, Kuznetsov SG, Court DL.** Recombineering: a homologous recombination-based method of genetic engineering. *Nat Protoc*. 2009;4:206–223.
33. **Sawitzke JA, Thomason LC, Costantino N, Bubunenko M, Datta S, Court DL.** Recombineering: in vivo genetic engineering in E. coli, S. enterica, and beyond. *Methods Enzymol*. 2007;421:171–199.
34. **Yu D, Sawitzke JA, Ellis H, Court DL.** Recombineering with overlapping single-stranded DNA oligonucleotides: testing a recombination intermediate. *Proc Natl Acad Sci USA*. 2003;100:7207–7212.
35. **Chen J, Zong CS, Wang LH.** Tissue and epithelial cell-specific expression of chicken proto-oncogene c-ros in several organs suggests that it may play roles in their development and mature functions. *Oncogene*. 1994;9:773–780.
36. **Matsushime H, Shibuya M.** Tissue-specific expression of rat c-ros-1 gene and partial structural similarity of its predicted products with sev protein of Drosophila melanogaster. *J Virol*. 1990;64:2117–2125.
37. **Sonnenberg E, Gödecke A, Walter B, Bladt F, Birchmeier C.** Transient and locally restricted expression of the ros1 protooncogene during mouse development. *Embo J*. 1991;10:3693–3702.
38. **Tessarollo L, Nagarajan L, Parada LF.** c-ros: the vertebrate homolog of the sevenless tyrosine kinase receptor is tightly regulated during organogenesis in mouse embryonic development. *Development*. 1992;115:11–20.
39. **Yeung CH, Sonnenberg-Riethmacher E, Cooper TG.** Infertile spermatozoa of c-ros tyrosine kinase receptor knockout mice show flagellar angulation and maturational defects in cell volume regulatory mechanisms. *Biol Reprod*. 1999;61:1062–1069.
40. **Shum WW, Ruan YC, Da Silva N, Breton S.** Establishment of cell-cell cross talk in the epididymis: control of luminal acidification. *J Androl*. 2011;32:576–586.
41. **Scholzen T, Gerdes J.** The Ki-67 protein: from the known and the unknown. *J Cell Physiol*. 2000;182:311–322.
42. **Jun HJ, Johnson H, Bronson RT, de Feraudy S, White F, Charest A.** The oncogenic lung cancer fusion kinase CD74-ROS activates a novel invasiveness pathway through E-Syt1 phosphorylation. *Cancer Res*. 2012;72:3764–3774.
43. **Robaire B, Hermo L.** 1988 Efferent duct, epididymis, and vas deferens: structure, functions, and their regulation. In: Knobil E, Neill JD, eds. The physiology of reproduction. New York: Raven Press; 999–1080.
44. **Breton S, Tyszkowski R, Sabolic I, Brown D.** Postnatal development of H+ ATPase (proton-pump)-rich cells in rat epididymis. *Histochem Cell Biol*. 1999;111:97–105.
45. **Jiang FX, Temple-Smith P, Wreford NG.** Postnatal differentiation and development of the rat epididymis: a stereological study. *Anat Rec*. 1994;238:191–198.
46. **Yeung CH, Sonnenberg-Riethmacher E, Cooper TG.** Receptor tyrosine kinase c-ros knockout mice as a model for the study of epididymal regulation of sperm function. *J Reprod Fertil Suppl*. 1998;53:137–147.
47. **Yeung CH, Wagenfeld A, Nieschlag E, Cooper TG.** The cause of infertility of male c-ros tyrosine kinase receptor knockout mice. *Biol Reprod*. 2000;63:612–618.
48. **Xu B, Abdel-Fattah R, Yang L, Crenshaw SA, Black MB, Hinton BT.** Testicular lumicrine factors regulate ERK, STAT, and NFKB pathways in the initial segment of the rat epididymis to prevent apoptosis. *Biol Reprod*. 2011;84:1282–1291.
49. **Xu B, Yang L, Lye RJ, Hinton BT.** p-MAPK1/3 and DUSP6 regulate epididymal cell proliferation and survival in a region-specific manner in mice. *Biol Reprod*. 2010;83:807–817.
50. **Xu B, Yang L, Hinton BT.** The role of fibroblast growth factor receptor substrate 2 (FRS2) in the regulation of two activity levels of the components of the extracellular signal-regulated kinase (ERK) pathway in the mouse epididymis. *Biol Reprod*. 2013;89:48.
51. **Charest A, Wilker EW, McLaughlin ME, et al.** ROS fusion tyrosine kinase activates a SH2 domain-containing phosphatase-2/phosphatidylinositol 3-kinase/mammalian target of rapamycin signaling axis to form glioblastoma in mice. *Cancer Res*. 2006;66:7473–7481.